

# Origin of Ferromagnetism and Long-range Interactions of Cu in GaN: Chemical Bonding and Electronegativity Approaches

Seung-Cheol LEE,\* Jung-Hae CHOI and Kwang-Ryeol LEE

*Computational Science Center, Korea Institute of Science and Technology, Seoul 136-791*

Pil-Ryung CHA†

*School of Advanced Materials, Kookmin University, Seoul 136-702*

(Received)

The diluted magnetic semiconductors (DMS) used in microelectronics should exhibit ferromagnetism mediated by delocalized electrons. Only Mn-doped GaN has passed this requirement, although the Curie temperature of this materials is at most 170 K, which is substantially lower than room temperature. Therefore, the development of a novel DMS with a higher Curie temperature is still an important issue. Recently, the potential of Cu-doped GaN has been demonstrated both theoretically and experimentally. However, it is not clear why Cu shows ferromagnetism. Using first principles density functional calculations, this study shows that the onset of magnetism of Cu in GaN results from the tendency of electrons to leave *anti-bonding* states. The delocalized electrons, which can stabilize the ferromagnetic alignment of the Cu ions, are generated at the Fermi level due to the small difference in electronegativities between nitrogen and Cu ions. For comparison, localized electrons are formed in Mn-doped GaN due to the large difference in electronegativities. The difference in electronegativities between the anion and the transition-metal impurity is expected to be helpful in the design of new DMS materials.

PACS numbers: 31.15.Ar, 31.10.+z, 51.60.+a, 75.50.Pp

Keywords: Diluted magnetic semiconductor, Cu-doped GaN, First-principles calculation, Electronegativity

## I. INTRODUCTION

Diluted magnetic semiconductors (DMSs) are usually made by the substitutional alloying of the host semiconductor (SC) cation site with transition metals (TMs). The TMs are assumed to be uniformly dispersed in the host SC. When TMs substitutionally occupy cation sites, the *d* states of the TM hybridize with the *p* states of the neighboring host anions. This *p-d* hybridization results in strong magnetic interactions between localized spins and carriers in the host's valence band [1]. As a result, the system exhibits stable ferromagnetism, and the spin-polarized carriers are used for spin manipulation. To our knowledge, Mn-doped GaAs is the only DMS material to fulfill the abovementioned criteria [2]. However, this successful DMS material exhibits a low Curie temperature, which prohibits practical application of the material. Studies aimed at increasing the Curie temperature while maintaining the DMS properties using other host semiconductors have been performed. Although there have been some reports of high-temperature ferromagnetism, the origin of the ferromagnetism is still being

debated [3,4]. No conclusive evidence has been reported. Therefore, the discovery or design of a new DMS material is still an important issue in the research area of spintronics.

Recently, experimental studies of the ferromagnetism of Cu-doped GaN have been reported. Lee *et al.* [5] observed room-temperature ferromagnetism of Cu-implanted GaN thin films. According to their results, the magnetic moment of Cu was  $0.27 \mu_B$ , based on the M-H curve. They also found that due to the clustering of Cu atoms the ferromagnetism was sensitive to the annealing temperature. Seong *et al.* [6] observed ferromagnetism of Cu in GaN nanowires. In their experiment, the magnetic moment was  $0.86 \mu_B$  per Cu atom, and the Curie temperature was far above room temperature. Based on anomalous X-ray scattering and X-ray diffraction results, they claimed that the Cu atoms substitutionally occupied the Ga site. Theoretical calculations regarding the possibility of ferromagnetism of Cu-doped GaN have been also reported. Lee *et al.* [7,8] studied the valence band splitting of transition-metal-doped GaN and suggested that Co- or Cu-doped GaN was the most probable candidate for DMS applications. Similar results were reported by Wu *et al.* [9] They reported that Cu in GaN showed ferromagnetism and that the conduction carrier

\*E-mail: leesc@kist.re.kr;

†E-mail: cprdream@kookmin.ac.kr

was 100% spin polarized. Based on mean-field calculations, they predicted the Curie temperature to be 350 K.

Even though both experimental and theoretical results have demonstrated the ferromagnetism of Cu-doped GaN, the fundamental question has not been solved: why does Cu-doped GaN exhibit ferromagnetism whereas bulk Cu is non-magnetic? Furthermore, which is the more promising DMS material: Cu-doped GaN or Mn-doped GaN?

We have investigated the potential of Cu-doped GaN for DMS applications by using first-principles calculations. The onset of ferromagnetism originates from the tendency for the number of electrons in *anti-bonding* states to be reduced. The long-range *p-d* hybridization, which is crucial to DMSs, of Cu-doped GaN occurs due to small differences in the electronegativities of TM ions and nitrogen. Finally, due to the exchange holes, elements such as Cu, having *more-than-half-filled* *d*-electron states are superior to elements such as Mn, having *less-than-half-filled* *d*-electrons with regard to the long-range hybridization of the TM *d* states and the anion *p* states.

## II. CALCULATION METHOD

All calculations were performed using the plane-wave basis code, the Vienna Ab-initio Simulation Package (VASP) [10, 11], based on density-functional theory and using ultrasoft pseudopotentials [12]. The generalized gradient approximation (GGA) parameterized by Perdew and Wang [13] was used for the exchange-correlation potential. To enhance the magnetic moment and the magnetic energies, we adopted the interpolation formula proposed by Vosko, Wilk, and Nusair [14]. The Ga *3d* state was treated as a semi-core state. To obtain an accurate total energy within a few meV of the convergence error, we used an energy cutoff of 800 eV, and an  $8 \times 8 \times 8$  Monkhorst-Pack special k-point mesh [15] to integrate the first Brillouin zone. The geometry was fully relaxed as the quantum-mechanical force and the total energy were minimized. Although the ground-state structure of GaN is wurtzite, this calculation assumed that the crystal structure was a zinc blende one because a symmetry analysis is simpler than that for wurtzite. The authors also calculated the wurtzite structure and found a similar tendency in the zinc blende structure. The calculated lattice parameter of the zinc blend GaN was 4.533 Å, which is only 0.7% larger than that of the experimental value of 4.5 Å [16]. A  $2 \times 2 \times 2$  supercell containing 64 atoms was used for the single transition metal (TM) ion calculations, which corresponds to 3.125 *et al.* of the TM concentration. The TM ions, Cu and Mn, were assumed to occupy the Ga site substitutionally.

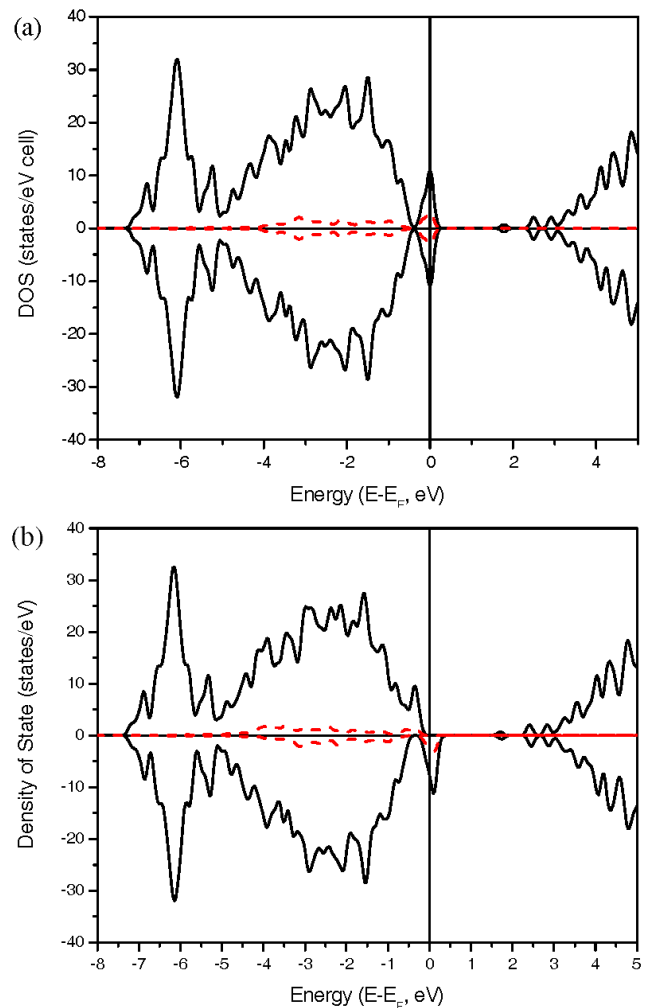


Fig. 1. Comparison of total DOS and Cu *d*-partial DOS of a paramagnetic and ferromagnetic solution of Cu-doped GaN: (a) paramagnetic phase (b) ferromagnetic phase. The solid lines and the dashed lines indicate the total and the partial DOS, respectively. The energy of the Fermi level was set to zero. The positive and the negative parts of each DOS correspond to the spin-up and the spin-down states, respectively. The Fermi level crosses the *anti-bonding*  $t_{2g}$  states, which were formed by hybridization between the N  $2p$  and the Cu  $3d$  states.

## III. RESULTS AND DISCUSSION

First-principles calculations were performed for Cu-doped GaN with and without spin degrees of freedom. In comparing the total energies between the magnetic and the non-magnetic solutions, that of the magnetic phase was 187 meV lower than that of the non-magnetic solution. The interatomic distance between Cu and N of the non-magnetic phase was 2.01 Å, which is slightly larger than the value of 1.96 Å for the Ga and N distance in pure GaN, due to the larger atomic radius of Cu. In the case of the magnetic phase, the interatomic distance between Cu and N was 0.0033 Å shorter than that of the

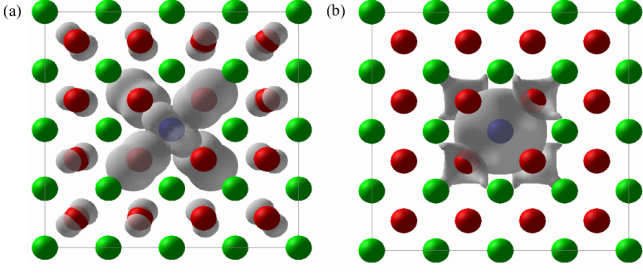


Fig. 2. Isosurface plots of the magnetization density: (a) Cu-doped GaN and (b) Mn-doped GaN. Green, red, and blue spheres represent Ga, N, and transition elements, respectively. The value of the isosurface was chosen at  $0.008$  electrons/ $\text{\AA}^3$ .

paramagnetic phase, which is a negligible difference.

Figure 1(a) shows the density of states (DOS) for the paramagnetic solution of Cu-doped GaN. The solid and dashed lines represent the total DOS and the Cu  $3d$  partial DOS, respectively. The Fermi level was set to *zero*. Since the Cu ion was assumed to substitutionally occupy the Ga site, the Cu ion experiences crystal field splitting in a tetrahedral environment, and as a result, degenerated  $d$  states of Cu are split into  $t_{2g}$  and  $e_g$  states [17]. The  $t_{2g}$  states then hybridize with the  $sp$  states of nitrogen and form *bonding* and *anti-bonding* states, leaving the  $e_g$  states as *non-bonding* states. The *bonding* states are mainly composed of  $p$  states originating from the anion  $p$  orbital while the *anti-bonding* states exhibit the  $d$  character from the  $d$  orbital of TM [18]. As seen in the figure, the Fermi level crosses the *anti-bonding*  $t_{2g}$  states. This situation is unfavorable for the electrons, and the system tends to reduce the number of electrons in the *anti-bonding* states. There are two ways to decrease the number of electrons in the *anti-bonding* states. One is a deformation of the crystal structure, such as Jahn-Teller distortion [19]. The other is a spontaneous spin splitting of the electrons, due to exchange interactions [20]. As mentioned before, the atomic distances between Cu and N with and without magnetization were the same. Thus, the Jahn-Teller mechanism does not occur. The latter mechanism, spontaneous magnetization, occurs in the Cu-doped GaN system. Fig. 1(b) shows the DOS for the ferromagnetic solution. As a result of spin polarization, the number of electrons in the *anti-bonding*  $t_{2g}$  state is drastically decreased from 3.2 for the paramagnetic phase to 0.8 electrons for the ferromagnetic phase. The spontaneous magnetization results in a 75% decrease in electrons in the *anti-bonding* state, which decreases the total energy of the spin-polarized system. The calculated total magnetic moment was  $2.0 \mu_B$ , which is consistent with other calculations [9].

The detection of magnetism is merely the first step in developing a novel DMS material. The next step is to examine the characteristics of the valence electrons at the Fermi level because a DMS should possess spin-polarized delocalized carriers. For example, if a material exhibits

strong ferromagnetic properties, but is simultaneously a magnetic insulator, this material will not be used in spintronics applications because there are no delocalized carriers for spin injection. The magnetic moment of Cu, as determined by projecting the wavefunction onto spherical harmonics, was estimated to be  $0.65 \mu_B$ . The remaining magnetic moment,  $1.35 \mu_B$ , was spread among the nitrogen atoms throughout the whole cell. In contrast, in the case of Mn-doped GaN, the projected magnetic moment was  $3.55 \mu_B$  while the total magnetic moment was  $4 \mu_B$ . The differences between the total and transition-metal magnetic moments were  $1.35$  and  $0.45 \mu_B$  for Cu- and Mn-doped GaNs, respectively. Therefore, approximately 90% of the magnetic moment of Mn-doped GaN was concentrated at the impurity atom while only 32% of the magnetic moment was concentrated at the transition metal impurity in Cu-doped GaN.

Figure 2 shows the isosurfaces of the magnetization density of Cu- and Mn-doped GaN. The magnetization density is defined as the charge density difference between the spin-up and the spin-down charge densities. The value of the isosurface was chosen at  $0.008$  electrons/ $\text{\AA}^3$ . The transition metal is represented by the blue sphere in the center of each figure. In the case of Cu (Fig. 2(a)), all of the nitrogen atoms in the calculation cell show a finite magnetization density whose spatial extent depends on the distance from the Cu ion. In contrast, in the case of Mn, which is shown in Fig. 2(b), the magnetization density is only found at the Mn atom and at the first nearest-neighbor anions. It should also be noted that most of the magnetization densities originate from the valence band top near the Fermi level.

Since the valence band top is composed of *anti-bonding* states between the transition metal  $t_{2g}$  states and the anion  $p$  states, the carriers in this system are holes. The mobility of holes is dominated by the characteristics of those states. The relative strength of the  $d$  character in the *anti-bonding* states, in turn, depends on the difference in the electronegativities of the transition metal element and the anion. The electronegativity of N is 7.3 eV while the electronegativities of Mn and Cu are 3.72 and 4.48 eV, respectively [21].

Schematic diagrams of the orbital hybridization that occurs when Mn or Cu bonds to N are shown in Fig. 3. In the case of Mn and N, whose difference in electronegativity is 3.58 eV, which is depicted in Fig. 3(a), the bond shows a stronger ionic character, and the *anti-bonding*  $t_{2g}$  state has a stronger  $d$  character, with the electrons being more localized at the transition ion itself. [18] If the electronegativity difference is small, the bond exhibits a stronger covalent character, and the *anti-bonding* state shows a weaker  $d$  character; as a result, the carriers show a more delocalized character, which is the case for Cu-doped GaN.

Furthermore, due to the existence of exchange holes, like-spin electrons do not shield each other from the nucleus or from electrons with different spins. Majority spins experience a higher effective nuclear charge and

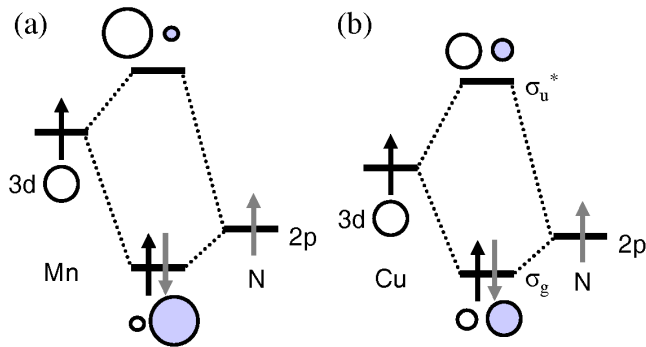


Fig. 3. Molecular orbital schematics of anion  $p$  and metal  $d$  hybridization. When two atoms form a bond, the atomic energy is split into *bonding* and *anti-bonding* states. The *bonding* and the *anti-bonding* states are located in the lower and upper part of the diagrams, respectively. (a) Hybridization of Mn and N, which is the case for a large difference in electronegativities (b) Hybridization of Cu and N, which is the case for a small difference in electronegativities.

will, therefore, move down in energy; thus, their associated spin orbitals are more contracted. The opposite effect works in minority spins, and the associated spin orbitals are expanded [22]. The electrons in the minority spin state can interact more with the anion  $p$  orbital. As a result, the  $p$ - $d$  hybridization may be stronger in the case of the Cu-doped system. In contrast, electrons in Mn only occupy the majority spin states, which are more contracted. The interaction between the Mn  $d$  states and the N  $p$  state is less effective, and the  $p$ - $d$  hybridization is weak. In the case of Mn-doped GaAs, which is the only known successful DMS material [23], the  $4p$  orbital in As is screened by the  $3p$  and the  $2p$  orbitals, and the spatial extent of As is much larger than that of N, whose  $2p$  electrons are not screened by the inner core and, thus, experience a higher effective nuclear charge. The strong  $p$ - $d$  hybridization observed in Mn-doped GaAs is due to the larger spatial extent of As while the strong  $p$ - $d$  hybridization of Cu-doped GaN results from the larger spatial extent of Cu.

#### IV. CONCLUSIONS

The electronic and the magnetic structure of Cu-doped GaN was studied using *ab-initio* calculations for designing a new DMS material. Cu-doped GaN satisfied the criteria for a successful DMS material: a local magnetic moment and long-range valence band splitting. In order to reduce the number of electrons in the *anti-bonding*  $t_{2g}$  states, the system spontaneously spin polarizes, which reduces the number of electrons in the Fermi level by 75%. The substitutions of Cu and Mn in a GaN host were compared; in Cu-doped GaN, the whole valence band of the nitrogen anion was split while in Mn-doped GaN, only the nearest-neighbor anions were split. Even

if Mn-doped GaN exhibits ferromagnetism, it cannot be used in DMS applications because its valence electrons are not spin polarized and cannot be used for spin injection.

The different behaviors of Cu and Mn in a GaN host can be explained by the differences in electronegativities between the transition metals and nitrogen and exchange holes. The differences in electronegativity determined the relative strength of the  $d$  states in the *anti-bonding*  $t_{2g}$  states. Since the electronegativity difference between Cu and N is smaller than that between Mn and N, the *anti-bonding* states showed a stronger  $p$  state character. Due to the efficient screening of the minority spin by the majority spin in Cu-doped GaN, the spatial extent of the *anti-bonding* state could be larger, which would enhance  $p$ - $d$  hybridization. Consideration of the differences in electronegativities between transition metal impurities and anions is expected to be useful in the design of new DMS materials.

#### ACKNOWLEDGMENTS

This work was partially supported by the KIST project for the "Development of Materials Design Technique at Molecular Scale using Massive Computation" under Contract Number 2E20640 (S.C.L, J.H.C, and K.R.L) and partially supported by the 2007 research fund of Kookmin University(P.R.C.). The calculations were performed using the KIST grand supercomputer and the UoSPCC-II system of the Seoul Parallel Computation Center at the University of Seoul.

#### REFERENCES

- [1] J. K. Furdyna, J. Appl. Phys. **64**, R29 (1988).
- [2] H. Ohno, J. Magn. Mater. **200**, 110 (1999).
- [3] S. A. Chambers, Surf. Sci. Rep. **61**, 345 (2006).
- [4] C. Liu, F. Yun and H. Morkoç, J. Mater. Sci.: Mater. El. **16**, 555 (2005).
- [5] J.-H. Lee, I.-H. Choi, S. Shin, S. Lee, C. Whang, S.-C. Lee, K.-R. Lee, J.-H. Baek, K. H. Chae and J. Song, Appl. Phys. Lett. **90**, 032504 (2007).
- [6] H. K.Seong, J. J. Kim, S.-C. Lee, S. R. Kim, J.-Y. Kim, T.-E. Park and H.-J. Choi, Nano Lett. **7**, 3366 (2007).
- [7] S.-C. Lee, K.-R. Lee and K.-H. Lee, Solid State Phenom. **124-126**, 847 (2007).
- [8] S.-C. Lee, K.-R. Lee and K.-H. Lee, J. Magn. Mater. **310**, e732 (2007).
- [9] R. Q. Wu, G. W. Peng, L. Liu and Y. P. Feng, Appl. Phys. Lett. **89**, 062505 (2006).
- [10] G. Kresse and J. Hafner, Phys. Rev. B **47**, 558 (1993).
- [11] G. Kresse and J. Furthmuller, Comp. Mater. Sci. **6**, 15 (1996).
- [12] D. Vanderbilt, Phys. Rev. B **41**, 7892 (1990).
- [13] J. P. Perdew and Y. Wang, Phys. Rev. B **45**, 13244 (1992).

- [14] S. H. Vosko, L. Wilk and M. Nusair, *Can. J. Phys.* **58**, 1200 (1980).
- [15] H. J. Monkhorst and J. D. Pack, *Phys. Rev. B* **13**, 5188 (1976).
- [16] T. Lei, T. D. Moustakas, R.J. Graham and S.J. Berkowitz, *J. Appl. Phys.* **71**, 4933 (1992).
- [17] S. Blundell, *Magnetism in Condensed Matter* (Oxford University Press, New York), p. 47.
- [18] R. Hoffmann, *Solids and Surfaces: A Chemist's View of Bonding in Extended Structures* (Wiley-VCH, New York, 1988), p. 58.
- [19] H. A. Jahn and E. Teller, *Proc. Roy. Soc. London A* **161**, 220 (1937).
- [20] R. Dronskowski, K. Korczak., H. Lueken and W. Jung, *Angew. Chem. Int. Ed.* **41**, 2528 (2002).
- [21] R. G. Pearson, *Inorg. Chem.* **27**, 734 (1988).
- [22] R. Dronskowski, *Computational Chemistry of Solid State Materials* (Wiley-VCH, Weinheim, 2005), p. 97.
- [23] T. Dietl, H. Ohno, J. Cibert and D. Ferrand, *Science* **287**, 1019 (2000).